Accuracy of a Multiprobe Conformal Sensor in Estimating the Dielectric Constant in Deep Biological Tissues

Andrea Michel, *Student Member, IEEE,* Konstantinos Karathanasis, *Member, IEEE,* Paolo Nepa, *Member, IEEE,* and John L. Volakis, *Fellow, IEEE*

***Abstract*— A theoretical analysis is presented on the accuracy of a novel method to extract the dielectric constant of deep tissues. The method exploits the variations of the electric fields on the surface of a multilayer dielectric scattering model and their dependence on dielectric properties of the deep tissues. The dielectric constant at a specific depth is expressed as a linear combination of the surface electric field samples. Critical parame-ters that affect the accuracy are determined through a numerical study, and basic guidelines for sensor design optimization are provided, using an emulation of a human torso. It is concluded that accuracies with errors <3% can be achieved, demonstrating the efficacy of the method and proposed representation.**

***Index Terms*— Biomedical sensor, human health monitoring, tissue dielectric properties, wearable electronics.**

I. Introduction

MAGNETIC resonance Imaging (MRI), X-ray and Computerized Tomography (CT) are the most used surgery-free technologies to detect tumors and produce deep tissues images. Nonetheless, they are not able to provide real time human tissue characterization, as they are not body-worn systems. Also, they are expensive and not portable for use in rural areas or in the field for emergency diagnostics.

There is, of course, a strong need to develop low cost health monitoring devices. Devices such as those in [1], [2] pursue monitoring of breathing, heart rate, temperature or blood pressure monitoring. But these devices are not suitable for imaging as they penetrate only few cm within the skin.

Toward this goal, a new on-body health-monitoring sensor was proposed in [3]–[5]. This is a multi-probe sensor operating at 40MHz, providing penetration depth of 10-15 cm within the human body. Therefore, it can be used to sense deep tissue dielectric properties. Specifically, the dielectric constant of the medium of interest is calculated using a linear combination of the S-parameters measured at the sensor's passive probes. In this way, the classic inverse-scattering approach is avoided. That is, we avoid the solution of ill-posed matrices [6]–[9]. As claimed in [4], experimental results have demonstrated that the proposed method can provide dielectric constant estimation with errors less than 11%. However, this level of accuracy is not sufficient. Therefore, there is a need to improve imaging accuracy (dielectric constant prediction) down to 2-3% by optimizing the sensor in [4].

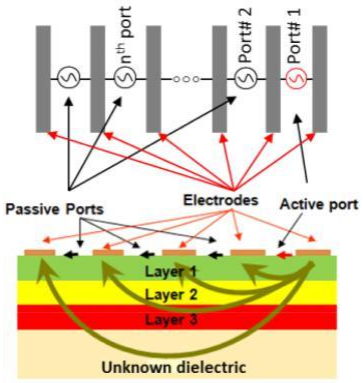

Fig. 1. Top and lateral view of the multi-probe sensor. The electric field force lines inside the medium are also shown.

In this paper, a numerical study is performed to better assess the algorithm's prediction capability and determine critical parameters that affect its accuracy. Specifically, a stratified dielectric medium is used to model the human torso. The probe sensor is a linear arrangement of transmitting and receiving ideal dipoles sources or probes (see Fig. 1). For a specific excitation, a spectral domain Green's function is used to calculate the received fields at the probe locations. The dielectric constant at a specific depth inside the torso is then expressed as a weighted sum of the computed electric field samples. General guidelines for sensor design optimization are extracted and employed to achieve dielectric constant estimation with better than 3% accuracies.

The paper is organized as follows. In Section II the overall imaging sensor concept is briefly described. The proposed model and numerical approach used to estimate the deep tissues dielectric constant is then presented in Section III. In Section IV, we discuss the results and provide guidelines for further sensor improvement.

Manuscript received XXX.

A. Michel and P. Nepa are with the Department of Information Engineering, University of Pisa, Pisa 56122, Italy (e-mail: andrea.michel@iet.unipi.it; p.nepa@iet.unipi.it).

K. Karathanasis was with the Electroscience Laboratory, Ohio State University, Columbus, OH 43212 USA. He is now with the School of Electrical and Computer Engineering, National Technical University of Athens, Athens 15780, Greece (e-mail: kkarathanasis@biosim.ntua.gr).

J. Volakis is with the ElectroScience Laboratory, Ohio State University, Columbus, OH 43212 USA (e-mail: volakis.1@osu.edu)

Color versions of one or more of the figures in this paper are available online at http://ieeexplore.ieee.org.

Digital Object Identifier 10.1109/JSEN.2015.2439032

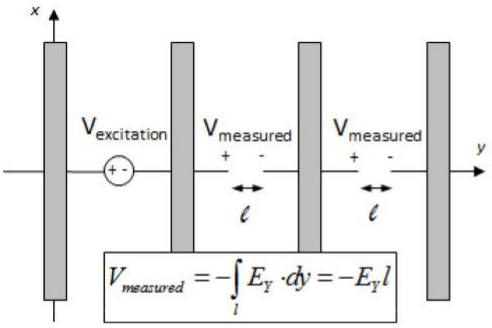

Fig. 2. Schematic representation of the relation between electric field and voltage (which is related to the S-parameters).

II. Sensor Overview

The sensor concept to estimate the dielectric constant has been presented in [3]–[5], and is briefly summarized below. The proposed sensor consists of a finite set of 17 electrodes, as in Fig. 1.

The overall sensor size is 16 × 10 cm^2 and is designed for human torso applications. The proposed sensor size and number of electrodes were chosen to ensure sufficiently large dynamic range in the values of $S_{i,1}$ [5]. Only one port (a port is the gap between two electrodes) is fed by a 40MHz input signal, while the rest are used for receiving the radiated fringing field after propagation and attenuation into the tissues. Specifically, the S-parameters are collected from the passive ports, denoted as $S_{i,1}$, where i = 2, 3,….16. Port #1 is always active and the others terminated with a matched load. Using the collected $S_{i,1}$ parameters, the dielectric constant (ε_r) is then represented by a weighted sum of the measured scattering parameters via the relation

$$\varepsilon_r = \sum_{i=2}^{N} w_{i-1} S_{i,1} \tag{1}$$

The coefficients w_i in (1) are computed to minimize the error in approximating ε_r for a set of known configurations. That is, they are determined by enforcing (1) for several combinations of assigned outer tissue layers and known values of the inner layer dielectric constant [5]. This process generates a system of equations solved via a least squares method to extract the coefficients w_i in (1). Measurements given in [5] confirmed the effectiveness of the representation (1). However, for the selected sensor, the estimation error was up to 11%. Below, we examine the sensor length and required number of probes to obtain accuracies with error lower than 2-3%.

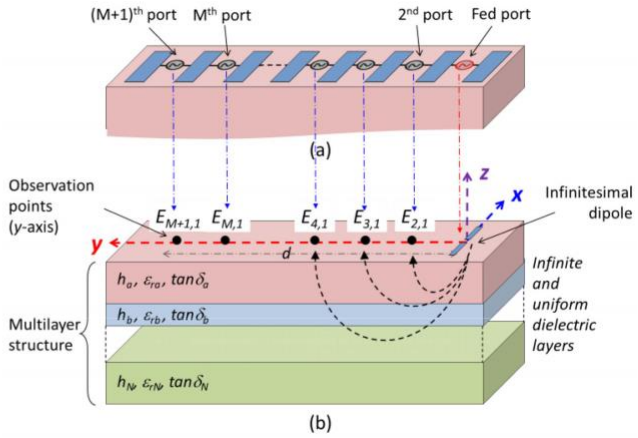

Fig. 3. (a) Actual multi-probe sensor with ports. (b) Multi-layer model for dipole excitation simulation.

III. Layered Model

To optimize the sensor length and number of probes for minimal error, we consider an ideal dipole excitation depicted in Fig. 3(b). The excited infinitesimal dipole is oriented along the x -direction. In practice, we measure the voltage between the probes. The latter is related to the electric field, as shown in Fig. 2. Thus, instead of measuring the fields as the voltage between two electrodes, we will simply use the x -directed electric fields along the y-axis (see Fig. 3(b)). These fields are, of course, proportional to the voltage between the electrodes (Fig. 2) and will be used to represent the $S_{i,1}$ values in (1).

We specifically chose to examine the surface fields up to 30cm away from the dipole excitation. That is, we examined sensor lengths up to 30cm.

To compute the dipole excitation fields in presence of the multilayer medium, we used the spectral representation of the Green's functions [10]. Using this approach, the electric fields for the TE and TM components are given by (2) and (3), as shown at the bottom of this page. In these expressions, $k_1 = \omega\sqrt{\mu_1\varepsilon_1}$ and $Z_1 = \sqrt{\mu_1/\varepsilon_1}$ refer to the wavenumber and intrinsic impedance of region 1, respectively [10]. Also, $k_{1z} = \sqrt{k_1^2 - k_\rho^2}$, where $k_\rho^2 = k_x^2 + k_y^2$. Further, R_{TE} and R_{TM} are the TE and TM plane wave reflection coefficients of an impinging plane wave at the interface [10], [14].

Since both R_{TE} and R_{TM} are functions of k_ρ , the double integral can be reduced to a single integral by invoking the well-known Sommerfeld and Weyl identities [10]. For brevity, the final integral expression is given in (4), as shown at the bottom of this page, for the dominant field component, E_x^{TE}.

$$\mathbf{E}_{TM} = -\frac{Z_1}{2k_1}\left(\frac{1}{2\pi}\right)^2 \int_{-\infty}^{\infty}\int_{-\infty}^{\infty}\left(\left[\frac{\hat{x}k_x k_{1z} + \hat{y}k_y k_{1z}}{k_1^2 - k_{1z}^2}\right] + \hat{z}\right) k_x (1 - R_{TM})\tilde{J}_x(k_x, k_y)\, e^{-jk_{1z}z} e^{j(k_x x + k_y y)} dk_x dk_y \tag{2}$$

$$\mathbf{E}_{TE} = -\frac{k_1 Z_1}{2}\left(\frac{1}{2\pi}\right)^2 \int_{-\infty}^{\infty}\int_{-\infty}^{\infty}\left(\frac{\hat{x}k_y - \hat{y}k_x}{k_1^2 - k_{1z}^2}\right) k_y (1 + R_{TE})\tilde{J}_x(k_x, k_y)\frac{e^{-jk_{1z}z}}{k_z} e^{j(k_x x + k_y y)} dk_x dk_y \tag{3}$$

$$E_x^{TE}(\rho, \varphi, z) = jk_1 Z_1 \frac{I_0}{8\pi}\sin^2\varphi \int_{-\infty}^{\infty}\left[-\frac{1}{\rho}\mathrm{H}_0^{(2)}(k_\rho\rho) + \left(\frac{2}{k_\rho\rho^2} - k_\rho\right)\mathrm{H}_1^{(2)}(k_\rho\rho)\right](1 + R_{TE})\frac{e^{-jk_{1z}z}}{k_z} dk_\rho \tag{4}$$

TABLE I

NOMINAL VALUES AND VARIATION RANGE OF THE TISSUE ELECTRICAL PROPERTIES AND THICKNESSES [15]

Tissue	Dielectric Constant (ε_r)	Loss tangent ($tan\delta$)	Thickness (h) [cm]
Skin	93.73 ± 10%	2.17 ± 10%	0.3 ± 10%
Fat	7.33 ⊥ 10%	2.09 ⊥ 10%	1.5 ⊥ 10%
Muscle	82.57 ± 10%	3.64 ± 10%	1.5 ± 10%
Bone	26 ± 10%	1.55 ± 10%	2.0 ± 10%
Lung	65 ± 40%	2.65 ± 20%	15 ± 20%

Using these representations, the fields arecomputed on the medium's surface along the *y*-axis in Fig. 3(b). Thus, only the field component parallel to the dipole orientation is used.

As is well known, direct numerical computation of Sommerfeld's integral is time-consuming and computationally expensive. This is due to the oscillatory and slowly decaying nature of the integrands, especially whenever the source and observation points are on the same interface [11], [12]. Indeed, several techniques have been proposed in the literature to numerically evaluate Sommerfeld's integral.

Similarly to [10]–[14], we invoke Cauchy's theorem to deform the original path of integration off the real axis and avoid difficulties associated with integrand singularities along the real axis of integration [10]–[13]. Specifically, we decided to split the integration path γ into three paths, $\gamma_1 = (-\infty - j\,a,\ a - j\,a)$, $\gamma_2 = (a - j\,a,\ a + j\,a)$ and $\gamma_3 = (a + j\,a,\ \infty + j\,a)$, where a is chosen equal to $0.8k_0$. Doing so, the fields can be computed on the interface and used to estimate the inner layer dielectric constant. Having the fields at the original probe locations, and given that $S_{i,1}$ is proportional to the computed x -directed electric field, denoted as $E_{i,1}$, we proceed to express $\boldsymbol{\varepsilon_r}$ as

$$\varepsilon_r = \sum_{i=2}^{M} w_i E_{i+1,1} \tag{5}$$

This can be rewritten as

$$[\varepsilon_r]_{1\times N} = [w]_{1\times M}\,[E]_{M\times N} \tag{6}$$

Here, [$\boldsymbol{\varepsilon}$r] is the vector representing the "known" dielectric constant at the chosen depth for each of the N simulated combinations of other layers parameters, {w} is the matrix containing the coefficients to be determined, M is the number of points where the electric field is computed or probed, and [E] contains the calculated surface electric field values. As in [5], since N M, (5) is solved via the least squares method to obtain {w}.

The accuracy of (5) will likely depend on:

1. Number, N, of random simulated combinations used to populate the $[E]_{M\times N}$ matrix in (6), and
2. Sensor length, and
3. Distance between sampling points.

As in [5], we chose to generate the system (6) using the parameter variations in Table I for each layer. Below we discuss the accuracy of (6) for predicting the dielectric constant of deep layers representing the lung.

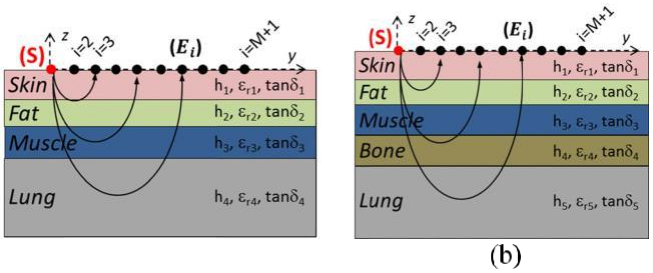

Fig. 4. Human torso equivalent model taking into account: (a) three and (b) four outer layers. Electric field propagation inside the medium is also sketched.

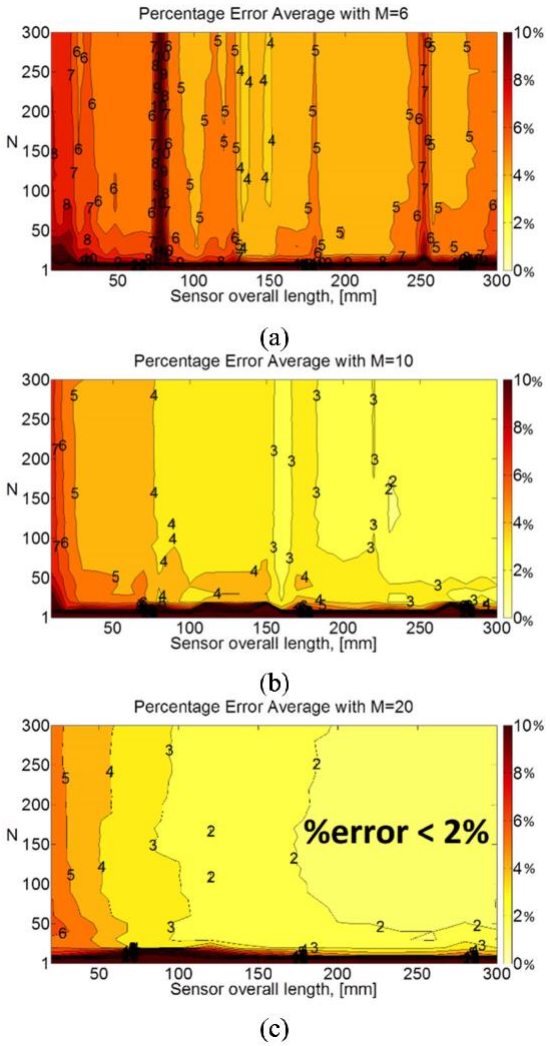

Fig. 5. Average percentage error in estimating $\boldsymbol{\varepsilon}$r4 (see Fig. 4(a)) when the sensor includes: (a) M = 6 probes, (b) M = 10 probes, and (c) M = 20 probes.

IV. NUMERICAL RESULTS

The accuracy of the proposed deep tissue dielectric constant extraction method was evaluated as a function of: (a) the sen-sor length, (b) the number of points where the electric field was probed, viz. number of field measurements points, and (c) the number of equations, N, used to populate the matrix {E} in (6). Two scenarios were considered, shown in Fig. 4. In one case, the torso model included 3 outer layers (skin, fat, and muscle) as depicted in Fig. 4(a). Of course, the proposed deep tissue

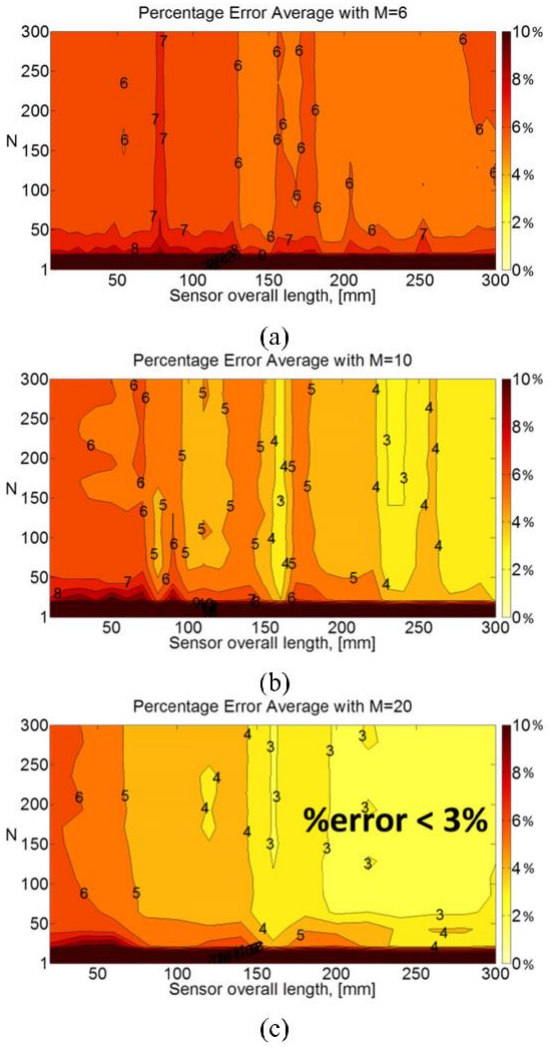

Fig. 6. Average percentage error in estimating ε_r5 (see Fig. 4(b)) when the sensor includes: (a) M = 6 probes, (b) M = 10 probes, and (c) M = 20 probes.

monitoring method must be able to provide accurate results for any arbitrary number of tissue layers and sensing depths. Therefore, to demonstrate the versatility of this method, we also considered a torso model with 4 outer layers (skin, fat, muscle, and bone). The latter scenario is depicted in Fig. 4(b).

To calculate the weight coefficients, $\{w_i\}$, we considered the parameter variations shown in Table I for each layer, leading to N = 2000 equations. After obtaining w_i, the average error of the approximation (6) was then obtained using different and random combinations of the top 3-4 layers. Specifically, we averaged the errors computed over 1000 random combinations of tissue electrical properties and thicknesses.

Fig. 5 and Fig. 6 show the average error in estimating the lung's dielectric constant for the scenarios depicted in Fig. 4(a) and Fig. 4(b), respectively.

A different set of weight coefficients, $\{w_i\}$, was computed and used for these two scenarios for several sampling points or probe number, M. Three different values of M were considered, M = 6, 10, and 20. The error for each of these M values was plotted in Figs. 5-6 for different number of equations, N. Specifically, the vertical axis of Fig. 5 and Fig. 6 refers to the number (N) of equations used to determine the w_i coefficients and the horizontal axis is the overall sensor length for M = 6, 10 and 20. As indicated to the right of the plots, deep red colors imply large errors (8-10%), whereas light yellow refers to low errors (<2%).

From the results in Figs. 5 and 6, we can extract the following guidelines for sensor design optimization:

- the electric field must be recorded across a sensing area that spans at least 20cm from the source point
- for a given sensor length, a larger number of probing points leads to greater accuracy
- increased accuracy is achieved as the matrix system used to solve for w_i increases in size.

Remarkably, for the scenario of Fig. 4(a), an average error of less than 2% may be achieved by (a) using at least 10 probes or field sampling points, (b) distributing the probes over a length at least 18-20cm, and (c) using at least N = 100 equations are needed for computing the coefficients w_i. For the scenario in Fig. 4(b), an average error of less than 3% was achieved by:
(a) using at least 20 probes, (b) distributing the probes across a length of at least 20cm, and (c) using at least N = 100 equations to compute the coefficients w_i. These scenarios provide consistent results for achieving an accuracy with error of 2-3% in extracting the lung's ε_r.

As would be expected, the accuracy of our expression (6) is lower for the case in Fig. 4(b), compared to that of Fig. 4(a).

V. Conclusion

A theoretical analysis was presented to assess the accuracy of a novel method for extracting the dielectric constant, ε_r, of deep human tissue. To do so, the human torso was modeled as a stratified dielectric medium and the electric field distribution on its surface was computed using a custom numerical code. A key aspect of the extraction method was the representation of ε_r as a linear combination of the surface electric field samples. The paper presented guidelines for sensor design optimization. It was concluded that the deep tissue's dielectric constant can be estimated with errors lower than 3%, at almost any arbitrary depth. Future steps will include: (a) further experimental verification, and (b) expan-sion of the proposed method to provide 2-D localization of the dielectric constant aimed at developing an imaging method for the torso cross-section that involves additional complexity.

References

[1] R. Paradiso, G. Loriga, and N. Taccini, "A wearable health care system based on knitted integrated sensors," *IEEE Trans. Inf. Technol. Biomed.*, vol. 9, no. 3, pp. 337–344, Sep. 2005.

[2] T. Yilmaz and Y. Hao, "Compact resonators for permittivity reconstruction of biological tissues," in *Proc. 30th URSI General Assembly Sci. Symp.*, Aug. 2011, pp. 1–4.

[3] S. Salman, L. Z. Lee, and J. L. Volakis, "A wearable wrap-around sensor for monitoring deep tissue electric properties," *IEEE Sensors J.*, vol. 14, no. 8, pp. 2447–2451, Aug. 2014.

[4] S. Salman, Z. Wang, E. Colebeck, A. Kiourti, E. Topsakal, and J. L. Volakis, "Pulmonary edema monitoring sensor with integrated body-area network for remote medical sensing," *IEEE Trans. Antennas Propag.*, vol. 62, no. 5, pp. 2787–2794, May 2014.

[5] S. Salman, D. Psychoudakis, and J. L. Volakis, "Determining the relative permittivity of deep embedded biological tissues," *IEEE Antennas Wireless Propag. Lett.*, vol. 11, pp. 1694–1697, 2012.

[6] J. D. Shea, P. Kosmas, S. C. Hagness, and B. D. Van Veen, "Three-dimensional microwave imaging of realistic numerical breast phantoms via a multiple-frequency inverse scattering technique," *Med. Phys.*, vol. 37, no. 8, p. 4210, 2010.
[7] N. Joachimowicz, C. Pichot, and J.-P. Hugonin, "Inverse scattering: An iterative numerical method for electromagnetic imaging," *IEEE Trans. Antennas Propag.*, vol. 39, no. 12, pp. 1742–1753, Dec. 1991.
[8] A. H. Golnabi, P. M. Meaney, and K. D. Paulsen, "Tomographic microwave imaging with incorporated prior spatial information," *IEEE Trans. Microw. Theory Techn.*, vol. 61, no. 5, pp. 2129–2136, May 2013.
[9] L. Lo Monte, D. Erricolo, F. Soldovieri, and M. C. Wicks, "Radio frequency tomography for tunnel detection," *IEEE Trans. Geosci. Remote Sens.*, vol. 48, no. 3, pp. 1128–1137, Mar. 2010.
[10] J. L. Volakis and K. Sertel, *Integral Equation Methods for Electromagnetics*. Hertfordshire, U.K.: SciTech Publishing, Inc., 2012, sec. 2.7.
[11] P. B. Katehi and N. G. Alexopoulos, "Real axis integration of Sommerfeld integrals with applications to printed circuit antennas," *J. Math. Phys.*, vol. 24, no. 3, p. 527, Mar. 1983.
[12] A. Alparslan, M. I. Aksun, and K. A. Michalski, "Closed-form Green's functions in planar layered media for all ranges and materials," *IEEE Trans. Microw. Theory Techn.*, vol. 58, no. 3, pp. 602–613, Mar. 2010.
[13] Z. H. Firouzeh, G. A. E. Vandenbosch, R. Moini, S. H. H. Sadeghi, and R. Faraji-Dana, "Efficient evaluation of Green's functions for lossy half-space problems," *Prog. Electromagn. Res.*, vol. 109, pp. 139–157, 2010.
[14] W. C. Chew, *Waves and Fields in Homogenous Media*. New York, NY, USA: Wiley, 1999, sec. 2.1.
[15] D. Andreuccetti, R. Fossi, and C. Petrucci. (1997). *An Internet Resource for the Calculation of the Dielectric Properties of Body Tissues in the Frequency Range 10 Hz–100 GHz*. [Online]. Available: http://niremf.ifac.cnr.it/tissprop/

Andrea Michel received the B.E., M.E. (*summa cum laude*), and Ph.D. degrees in telecommunications engineering from the University of Pisa, Pisa, Italy, in 2009, 2011, and 2015, respectively. In 2014, he was a Visiting Scholar with the ElectroScience Laboratory, The Ohio State University, Columbus, OH, USA. During this period, he has been involved in research on a theoretical analysis on the accuracy of a novel technique for deep tissue imaging. He is currently a Post-Doctoral Researcher in Applied Electromagnetism with the Microwave and Radiation Laboratory, Department of Information Engineering, University of Pisa. His current research topics focus on the design of integrated antenna for communication systems and planar antennas for near field UHF–RFID readers.

Dr. Michel was a recipient of the Young Scientist Award from the International Union of Radio Science, Commission B, Beijing, China, in 2014, and Gran Canaria, Canary Islands, in 2015.

Konstantinos Karathanasis was born in Greece in 1982. He received the Diploma degree in electrical and computer engineering from the University of Patras, Greece, in 2005, and the M.Sc. and Ph.D. degrees from the Interuniversity Postgraduate Programme on Biomedical Engineering, in 2008 and 2010, respectively. In 2011, he joined the School of Electrical and Computer Engineering, University of Cyprus, where he served as a visiting academic for two years. In 2013, he conducted post-doctoral research at the ElectroScience Laboratory, The Ohio State University. Since 2014, he has been with the Biomedical Simulations and Imaging Laboratory, School of Electrical and Computer Engineering, National Technical University of Athens. He has co-authored over 20 papers published on international journals and conference proceedings. His research interests include antenna theory and design for biomedical applications, body sensor networks, arithmetic and experimental dosimetry, biomedical imaging techniques, and metamaterials.

Paolo Nepa received the Laurea (Ph.D.) (*summa cum laude*) degree in electronics engineering from the University of Pisa, Italy, in 1990. Since 1990, he has been with the Department of Information Engi-neering, University of Pisa, where he is currently an Associate Professor. In 1998, he was with the Electro Science Laboratory (ESL), The Ohio State University (OSU), Columbus, OH, as a Visiting Scholar supported by a grant from the Italian National Research Council. At ESL, he was involved in research on efficient hybrid techniques for the analysis of large antenna arrays. He is also involved in the design of wideband and multiband antennas, mainly for base stations and mobile terminals of communication systems, as well as in the design of antennas optimized for near-field coupling and focusing. More recently, he is involved in channel characterization, wearable antenna design, and diversity scheme implementation, for body-centric communication systems. In the context of RFID systems, he is working on techniques and algorithms for UHF-tag localization and RFID-based smart shelves. His research interests include the extension of high-frequency techniques to electromagnetic scattering from material structures and its application to the development of radio propagation models for indoor and outdoor scenarios of wireless communication systems.

Dr. Nepa received the Young Scientist Award from the International Union of Radio Science, Commission B, in 1998.

John L. Volakis (S'77–M'82–SM'89–F'96) was born in Chios, Greece, in 1956. He received the B.E. (*summa cum laude*) degree from Youngstown State University, Youngstown, OH, USA, and the M.Sc. and Ph.D. degrees from The Ohio State University, Columbus, OH, USA, in 1979 and 1982, respectively.

He started his career with Rockwell International from 1982 to 1984. He is currently with Boeing Phantom Works. In 1984, he was appointed as an Assistant Professor with the University of Michigan (UM), Ann Arbor, MI, USA, where he became a Full Professor in 1994. He served as the Director of the Radiation Laboratory from 1998 to 2000. Since 2003, he has been the Roy and Lois Chope Chair Professor of Engineering with The Ohio State University, and also serves as the Director of the ElectroScience Laboratory. He has carried out research on antennas, medical sensing, computational methods, electromagnetic compatibility and interference, propagation, design optimization, RF materials and metamaterials, RFIDs, millimeter waves and terahertz, body-worn wireless technologies, and multiphysics engineering. His publications include eight books, including *Approximate Boundary Conditions in Electromagnetics* (IET, 1995), *Finite Element Methods for Electromagnetics* (Wiley-IEEE Press, 1998), *Antenna Engineering Handbook* (McGraw-Hill, 2007, 4th ed.), *Small Antennas* (McGraw-Hill, 2010), and *Integral Equation Methods for Electromagnetics* (SciTech, 2011). His papers include over 350 journal papers, more than 650 conference papers, and 25 book chapters. He has also written several well-edited course packs and has delivered short courses on antennas, numerical methods, and frequency-selective surfaces.

Dr. Volakis is a Fellow of the Applied Computational Electromagnetics Society and a member of the URSI Commissions B and E, and currently serves as the Chair of the USNC/URSI Commission B. He was a recipient of the UM College of Engineering Research Excellence Award in 1998, the UM Department of Electrical Engineering and Computer Science Service Excellence Award in 2001, the Ohio State University Clara and Peter Scott Award for his outstanding academic achievement in 2010, the IEEE Antennas and Propagation Society (AP-S) Distinguished Achievement Award in 2014, and the IEEE AP-S C-T Tai Educator Award. He was listed by ISI among the top 250 most referenced authors in 2004. His mentorship includes over 80 doctoral students/post-doctoral students in which 30 of them receiving best paper awards at international conferences. He was the President of the IEEE AP-S in 2004, and served on the AdCom of the IEEE AP-S from 1995 to 1998. He also served as an Associate Editor of the IEEE TRANS ACTIONS ON ANTENNAS AND PROPAGATION from 1988 to 1992, *Radio Science* from 1994 to1997, the *IEEE Antennas and Propagation Society Magazine* from 1992 to 2006, the *Journal of Electromagnetic Waves and Applications*, and *URSI Bulletin*. Furthermore, he served on the IEEE Wide and AP-S Fellows Evaluation Committee. In 1993, he chaired the IEEE AP-S Symposium and Radio Science Meeting in Ann Arbor, and Co-Chaired the same symposium in 2003 at Columbus.